Analysis of Performance Loss Through I&V Characteristics Curves of Photovoltaic Modules in the Dark.

Leonel A. C. Poltosi, Arno Krenzinger and Cesar W.M. Prieb

Laboratório de Energia Solar (LABSOL)/PPGE3M

Universidade Federal do Rio Grande do Sul, Porto Alegre RS (Brazil)

Abstract

The characteristic I-V curves under standard conditions constitute the most effective method for assessing the health status of a given photovoltaic (PV) module. These curves enable the determination of a module's maximum power output. Furthermore, an I-V curve measured under dark conditions also provides significant information regarding the quality of the PV module under investigation. Recent scientific literature has demonstrated the existence of easily applicable techniques for diagnosing performance degradation in full-cell PV modules connected entirely in series. However, the most widely commercialized PV modules nowadays utilize a half-cell design with a series-parallel connection scheme, which may exhibit a different response to these diagnostic techniques. This work presents observations concerning the variations in experimentally determined characteristic curves, obtained through dark measurements and the flash test, for a 530W half-cell module subjected to mechanical damage of progressive intensities.

Keywords: PV module, I-V dark, PV fault evaluation, PV diagnosis, V10, Damage assessment.

1. Introduction

Photovoltaic (PV) module manufacturers are substantially interested in the intense global growth in utilizing solar photovoltaic energy. Commercial aspects involving high efficiencies and low prices are maintaining product competitiveness. In this context, while PV modules have increased in size, the silicon wafers used for cell manufacturing and the module glass have become thinner to reduce cost and weight.

A recent study by Palmiotti et al. (2025) indicates premature failures, including glass breakage in double-glass modules (although this phenomenon also occurs with single-glass modules). Adding to this information is that the Solar Energy Laboratory at UFRGS has also observed a higher incidence of fractured cells during electroluminescence testing, preceding power determination measurements. As many microfractures in cells can occur during module transportation, installation, and use, it would be highly beneficial to have a diagnostic method to monitor the potential performance degradation of a module without transporting it to a specialized laboratory for power measurement.

Another recent publication by Smith and Colvin (2025) proposes a rapid and low-cost diagnostic technique for assessing module performance loss. This technique, referred to as V10, involves connecting the module, under dark conditions, to a low-energy-consumption current source set at 10 mA and measuring the resulting voltage. This technique, however, was tested only on crystalline silicon modules with full cells connected exclusively in series. Currently, the most widely commercialized PV modules utilize a half-cell configuration, combining series-parallel connections, and are identified as 'half-cell modules'.

The present work aims to demonstrate the feasibility of the V10 technique for Half-Cell modules by recording the variation in the dark I-V curve for a module subjected to successive mechanical impacts.

2. Dark I-V Curves

Various studies, such as those by King et al. (1997) and Bouzidia et al. (2012), have utilized dark I-V curve measurements of photovoltaic modules to determine parameters for electrical characteristic models. Spataru

10.18086/swc.2025.03.04 Available at http://proceedings.ises.org

et al. (2015) presented an extensive study for fault identification in modules by conducting a complementary analysis between dark and I-V curves under solar irradiance, demonstrating that these curves are highly sensitive to degradations in module quality.

When current is plotted on a linear scale, the dark I-V curve of a photovoltaic module exhibits little variation when the module loses power. However, the differences become more evident when the current is represented with a logarithmic scale. Figure 1, taken from Spataru et al. (2015), illustrates this effect in a study applying Potential-Induced Degradation (PID), which resulted in power losses up to 10.4%.

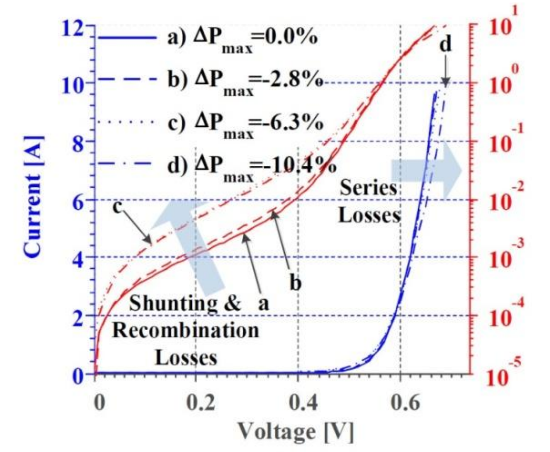

Figure 1. Differences in identifying power loss from dark I-V curves when the module current is displayed on a linear scale (blue) or a logarithmic scale (red). Source: Spataru et al. (2015).

Subsequently, Smith and Colvin (2025) proposed a method to monitor the health of photovoltaic modules, as cited in the introduction. The proposed technique resulted from an analysis of PV modules composed of 72 full cells connected exclusively in series. This design prevailed in module manufacturing for many years, where all cells are connected in series. Nevertheless, as new technologies allowed for an increase in monocrystalline silicon wafers, the half-cell circuit combining series-parallel associations has progressively replaced the conventional design.

3. Half-Cell Module Design

Half-cell PV modules feature improved performance characteristics compared to the former conventional design. Essentially, cells cut in half produce half the electric current, reducing power loss due to cell interconnection resistance by a factor of four. This innovation was accompanied by introducing multiple wires instead of ribbons to the inter-cell connections substring. The parallel connection of another identical substring compensates for the lower current. The most common design incorporates six substrings in a module, connected two-by-two in parallel, with each parallel pair sharing a bypass diode. The three resulting parallel pairs of substrings are then connected in series. Figure 2 illustrates the half-cell module design mentioned. This configuration also offers better tolerance to the adverse effects of partial shading, due to the increased probability that shading will affect only one of each of the parallel-connected substrings.

Besides the improved tolerance to partial shading, the analysis of Figure 2 leads to the conclusion that microcracks in the cells should also have a smaller impact on power output. A reduction in current within one cell of one of the six substrings will not affect the entire module shown in Figure 2(b) as severely as a current reduction in a single cell would affect the module in Figure 2(a).

The introduction of half-cell modules into the market was fast and they quickly replaced the conventional all-series cell design. According to Fischer et al. (2025), half-cell modules currently represent more than 95% of the market for silicon cell modules, and this design is likely to remain predominant in the coming years.

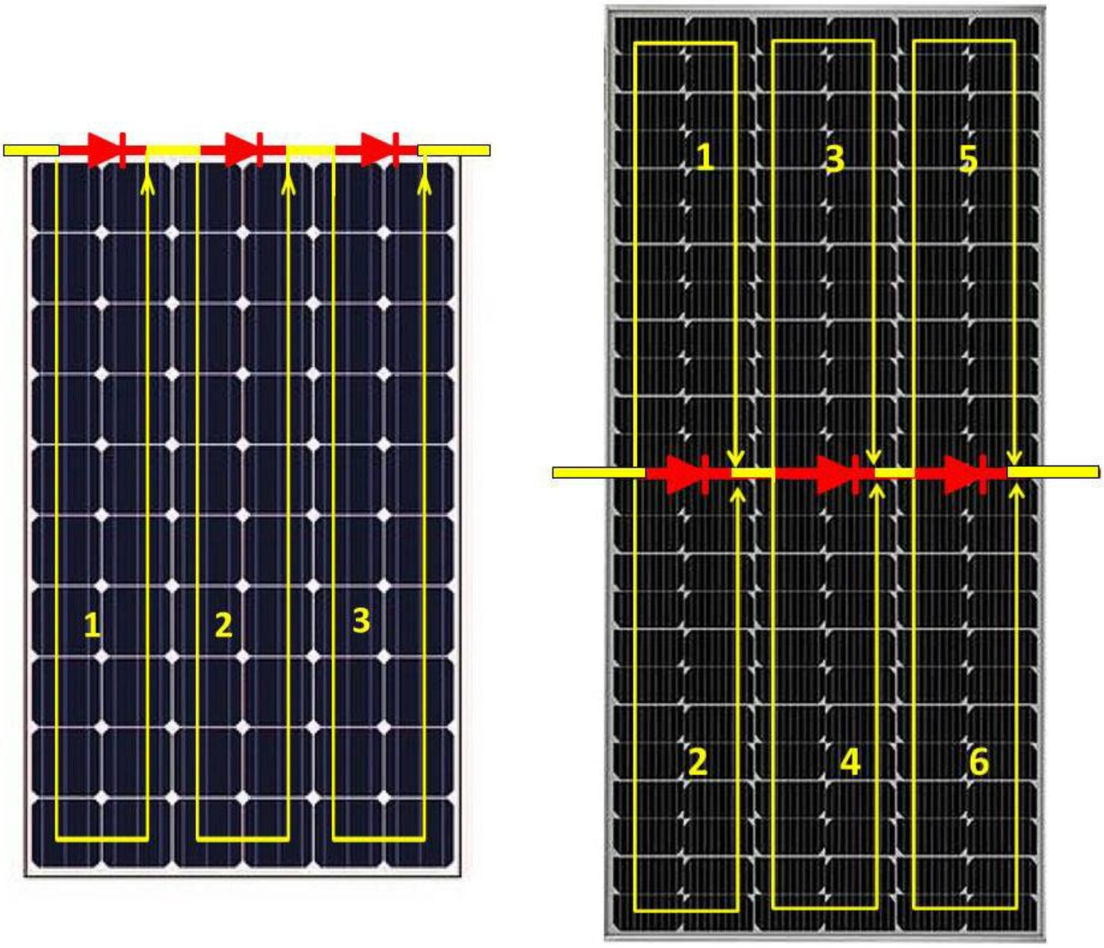

(a) (b)

Figure 2. Comparison between the conventional full-cell module design (a) and the half-cell module design (b). Yellow lines indicate the current path. In Figure (a), all cells are in series, and in Figure (b), each of the bypass diodes indicated in red shares two parallel strings.

In addition to electrical advantages, half-cell modules are also less susceptible to fracturing. A cell fracture simulation study developed by Bosco (2022) compared square and rectangular cells and demonstrated how rectangular cells may be less affected by fracturing from mechanical impacts. Figure 3 summarizes the simulation results to determine the fracture when applying the same load to PV modules, comparing full-cell and half-cell modules. In the half-cell case, the simulation also considered two orientation possibilities. These results add another advantage to the half-cell module design option.

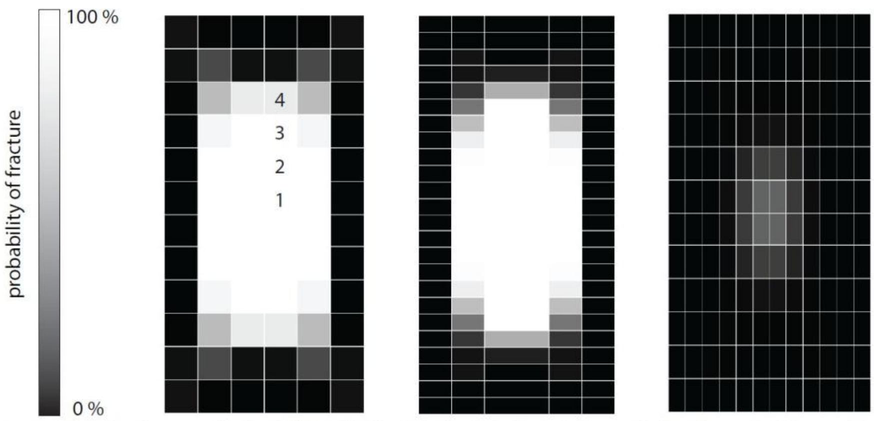

Figure 3: Simulated probability of fracture map to the (left to right) full-cell, half-cell short orientation and half-cell long orientation module, evaluated at 2800 Pa. Source Bosco (2022)

4. Experimental Methodology

The experiments reported in this work employed a 530 WP, monofacial module with 144 monocrystalline half-cells, 2.278 m lenght x 1.134 m wide. The experimental procedure consisted of placing the PV module inside the same dark chamber utilized either to acquire I-V curves under Standard Test Conditions (STC), as well as the dark I-V curves and electroluminescence tests.

The tests were executed in seven steps. The first step was conducted with the PV module free of any damage. In the subsequent steps, mechanical damage was inflicted through mechanical shocks (rubber mallet impacts) on the frontal and rear faces, corners and sides of the module. Damage was also produced by stepping on the front glass while the module was positioned horizontally.

As the objective is to identify the influence of imperceptible damage during visual inspection, care was taken to not break the module's glass. The following sequence of stages was executed at each step:

(a) Inflict one of the listed damages in a previously selected region. Efforts were made to distribute the damage across the module's substrings to evaluate the subsequent impact on electrical characterization;
(b) Verify that the region presents no visible damage;
(c) Obtain an EL image and evaluate the extent of microcracks;
(d) Perform a flash-test at STC to assess the impact on electrical characteristics;
(e) If the alteration of electrical characteristics is not significant, return to stage (a);
(f) Perform the dark I-V curve measurement of the module, noting its temperature;
(g) Proceed to the next step.

4.1 Solar Simulator

The LABSOL-UFRGS facility is equipped with a PASAN Large Area Pulsed Solar Simulator (LAPSS), model SunSim 3c, class A+A+A+. The LAPSS was installed in a tunnel with light collimators and coated with highly radiation absorbent material, adapted to accommodate PV modules with dimensions up to 2.4 m x 2.4 m. The LAPSS applies a flashlight with duration of 10 milliseconds. The irradiance of 1 kW/m^2 on the test plane is delivered by two xenon lamps filtered to adapt the produced light to the standard AM1.5 solar spectrum.

Even though the power measurement values of the PV module in the LAPSS have an absolute uncertainty in the order of 2.3 % (mostly due to the uncertainty in the calibration of the reference cell), the relative uncertainty when comparing the power between different flashes is much lower. Gasparin et al. (2016) evaluated the equipment's reproducibility by applying 31 consecutive I-V curve measurements on the same 450 W PV module at different positions on the same test plane. The results showed that the expanded relative expanded uncertainty for the value for those modules in the LABSOL-UFRGS LAPSS was only 0.15%. However, the module evaluated in the present work has larger dimensions, causing lower irradiance uniformity across its surface. Furthermore, the activities of plotting the dark curve and producing EL images also cause a decrease in module temperature uniformity. Finally, and likely the most critical factor: the short circuit current (I_{SC}) in those modules used in Gasparin et al. paper was about 9 A, while the module used in the present paper has I_{SC}= 13.5 A. This fact imposes the need for change the current full scale range in the electronic meter from 10A to 30A, which reduces the equipment's resolution by a factor of nearly 3. Therefore, it is reasonable to estimate the expanded relative uncertainty for power comparison at a value of 0.5%.

4.2 Photovoltaic Module Electroluminescence

Electroluminescence (EL) is a technique for assessing the integrity of photovoltaic cells. When a direct bias current is forced through the PV cells under dark, luminescence occurs due to the recombination of electrons with holes in the silicon. This process emits an intensity of infrared radiation that specific cameras can capture to form an image.

To obtain electroluminescence images, LABSOL employs a Canon Rebel T6 photographic camera with the infrared filter of the CCD unit previously removed. Images were acquired in the dark, with an exposure time of 15 seconds, an aperture of f/11, and an ISO sensitivity of 1600. The half-cell module was powered by a Regraton TopCon Quadro power supply, with a capacity of 600 V and 32 A, adjusted to deliver a forward-biased current to the PV module. The temperature during the EL image acquisition was monitored by the same PT100 sensor employed in the flash test with the solar simulator. Figure 4 shows the module fixed to the solar simulator tunnel structure to perform EL imaging.

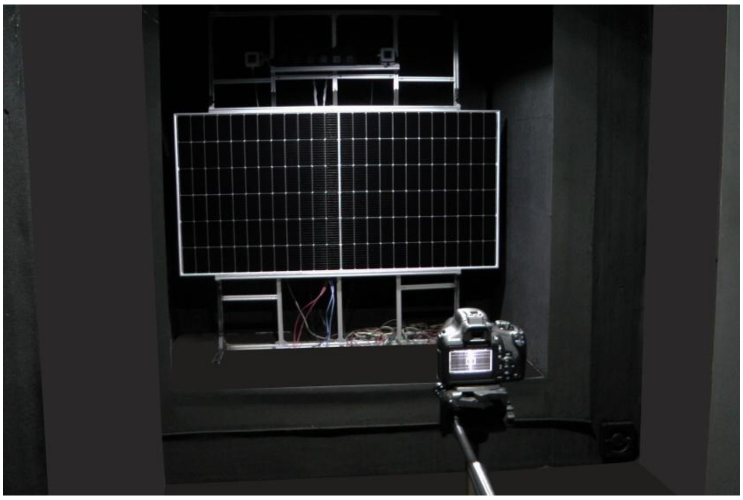

Figure 4: Module prepared for obtaining electroluminescence images in the sola simulator tunnel.

4.3 Dark I-V Curve Acquisition.

The experimental procedure for obtaining the Dark I-V curve consisted of placing the photovoltaic module under analysis inside the simulator tunnel, in the same rack used for the flash test. The measurement system is illustrated in Figure 5. The module is connected to a 400 W KEPCO bipolar DC source which applies a voltage ramp to the module's terminals for about three seconds. Two multimeters Keysight 34411A acquire simultaneously the voltage and current values. The current is measured via a calibrated 1 Ω/100 W shunt resistor. A software developed at LABSOL manages the acquisition and recording of the I V pairs through the GPIB communication interface. The module's temperature is monitored, allowing the subsequent application of temperature correction factors.

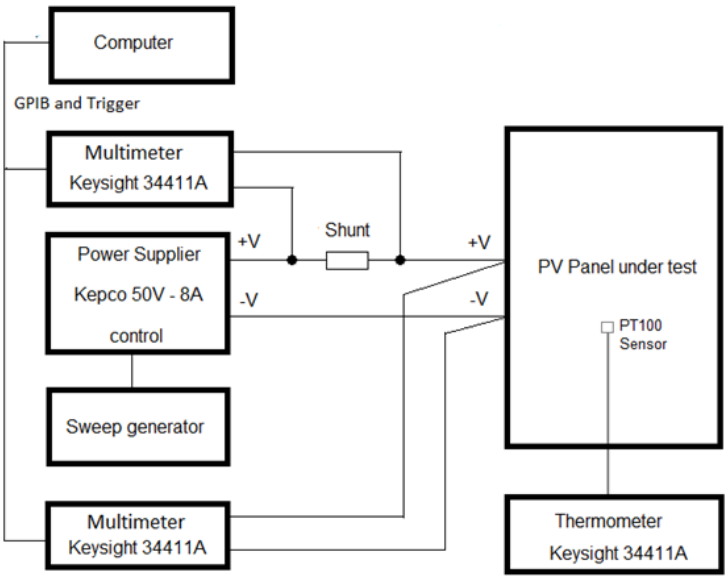

Figure 5: Schematic diagram of the dark I-V curve measurement system..

5. Results

In the first step, the module was not subjected to mechanical damage. A rubber mallet impact on the frontal face of the module was applied in the second and third steps. In the fourth step, a rubber mallet impact at the right superior corner was executed on the rear face. Finally, in the seventh step, the module was supported horizontally on four stands, and a 80 kg person walked across the front glass. Except for step 7, the damage was inflicted with the module positioned vertically on the solar simulator rack.

Figure 6(a) displays the EL image obtained in step 1, before mechanical impacts. The remaining images in Figure 6 show the result of the EL after the damage inflicted in each step between 2 and 6. It is observed that in steps 2 and 3, the EL reveals a dendritic-shaped multiple crack pattern in some cells, while in steps 4 through 6, belt-like patterns across the whole cell also occur. Figure 7 shows the EL image obtained in step 7, identifying the cell fractures sustained in each step.

The characteristic I-V curves measured with the solar simulator are presented in Figure 8. A superposition of the curves from the first six steps is noticeable, requiring the inclusion of a graph amplification between voltages from 32 V to 44 V for a more detailed observation and separation of the curves. Even with the amplification, the I-V curves for steps 1, 2, and 3 overlap, but steps 4, 5, 6, and 7 detach from the original curve. As mentioned in section 4.1, the relative uncertainty in power considered was 0.5%, which, when applied to a 530 W module, corresponds to ±2.7 W. The values of P_{MAX} extracted from the I-V curves corresponding to steps 1, 2, and 3 have differences smaller than this uncertainty.

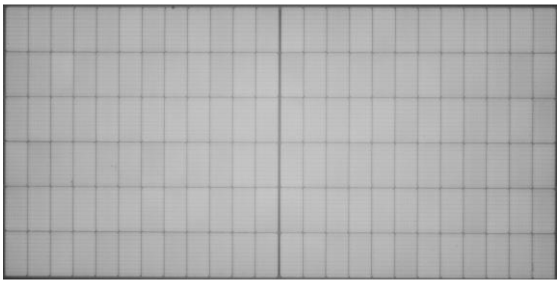

(a) STEP 1

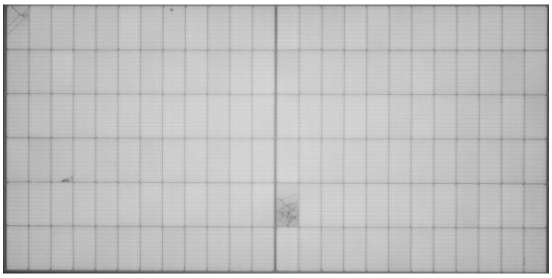

(b) STEP 2

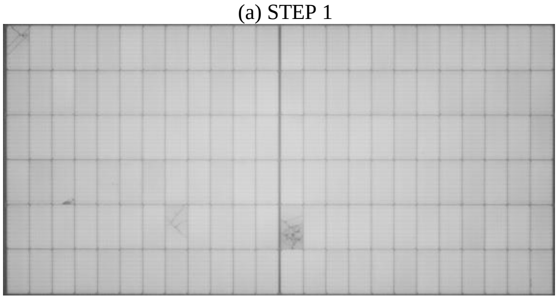

(c) STEP 3

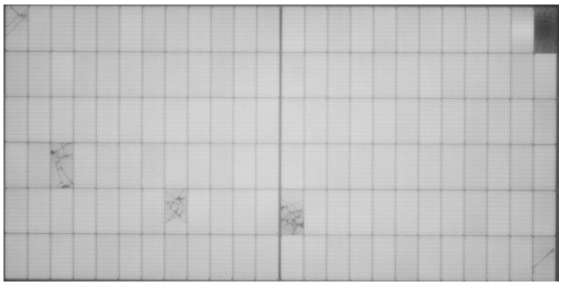

(d) STEP 4

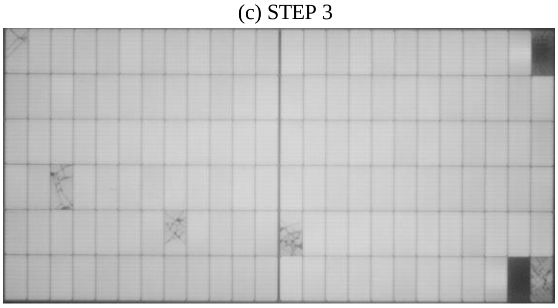

(e) STEP 5

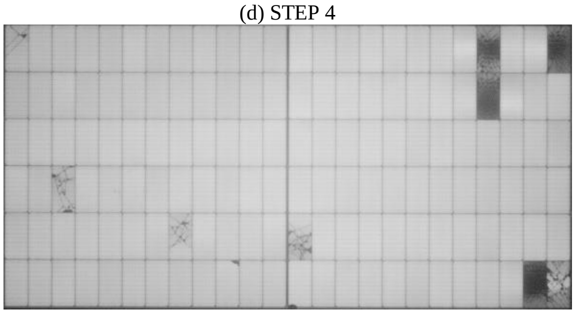

(f) STEP 6

Figure 6. EL images obtained in steps 1 through 6. (a) STEP 1; (b) STEP 2; (c) STEP 3; (d) STEP 4; (e) STEP 5; (f) STEP 6.

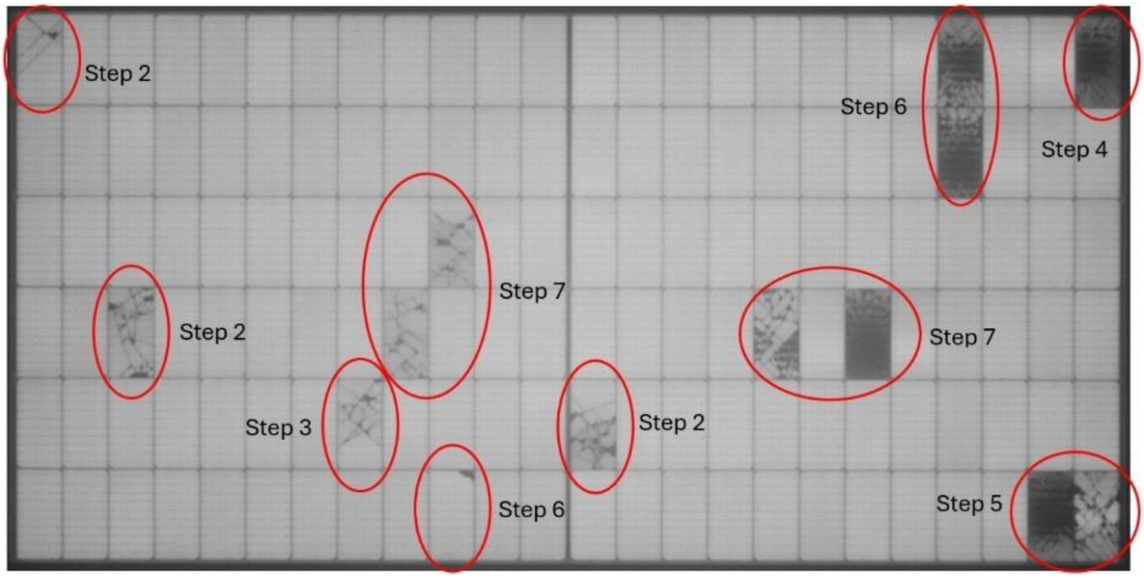

Figure 7 EL image obtained in step 7, indicating the damaged cells in each step.

The evaluation of the effects of the temperature on the half-cell module's dark I V curves were obtained experimentally. The undamaged PV module in Step 1 was heated and then subjected to natural cooling from 30 °C to 20 °C, with dark I V curve measurements taken sequentially at each variation of 0.5 °C. The V10 temperature correction coefficient was found to be -0.166 V/ºC.

The dark I-V curve measurements at every step were performed at temperatures close (within a few tenths of a degree) to 25 ºC. Nevertheless, before plotting the corresponding graphs, the data were corrected using the found temperature coefficient. Figure 9 displays the temperature corrected dark I-V curve plots, with the current on a logarithmic scale. The damage inflicted in step 3 was almost imperceptible when compared to step 2, involving only a cell with minimal damage, thus the dark I-V curves were practically superimposed. Figure 9 features an inset with an enlarged graph in the region between 30 V and 35 V. The V10 values varied from 24.56 V (step 1) to 31.84 V (step 7).

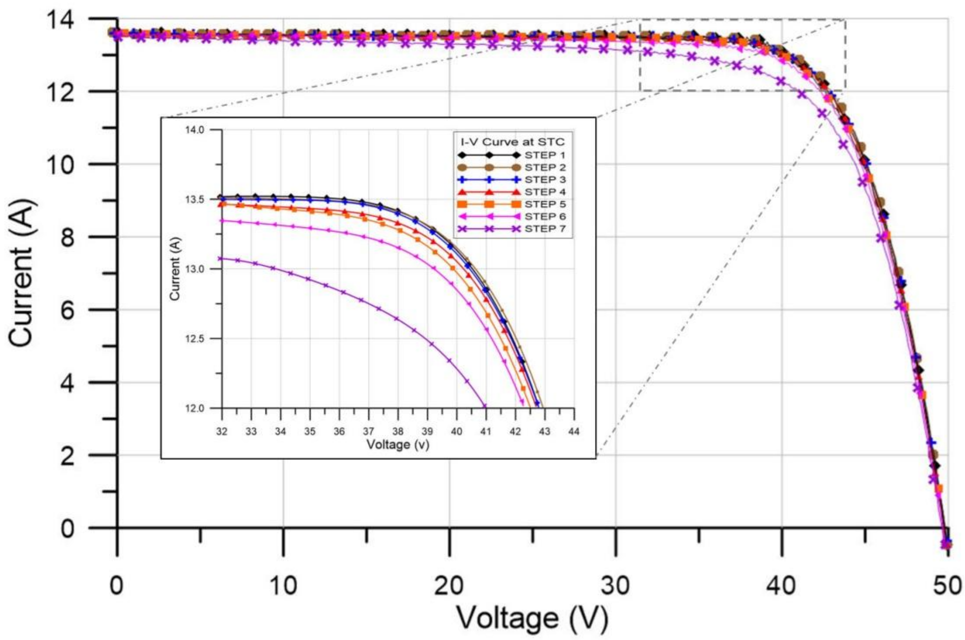

Figure 8: I-V curves obtained with the solar simulator after each damage step, indicating the impact of the inflicted damage on module performance at STC. The inset graph is an amplification of the interval between 32 V and 44 V.

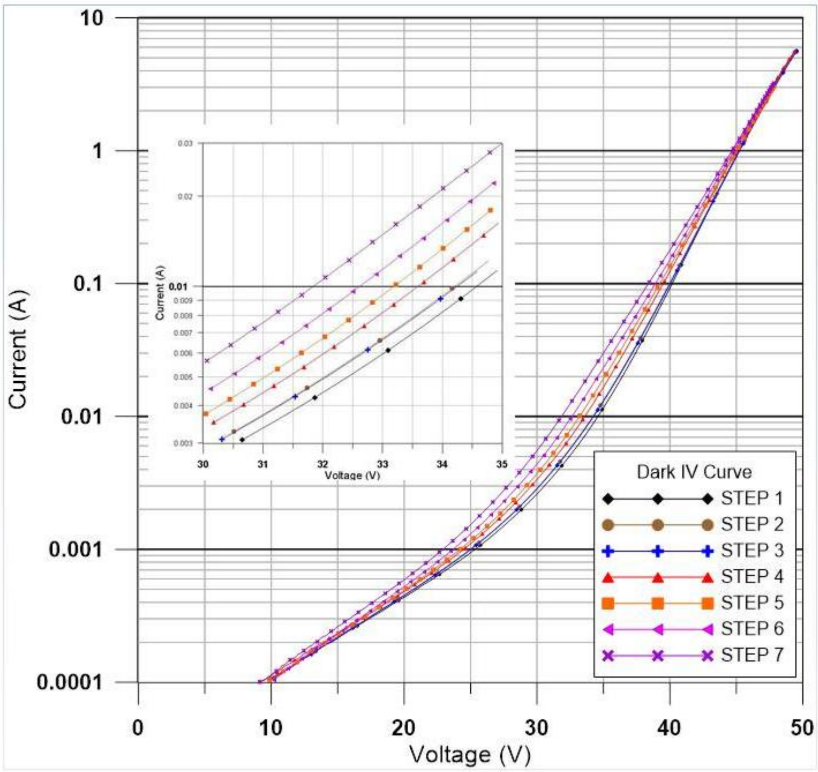

Figure 9: Dark I-V curves obtained after applying damage to the half-cell module in each step, with the current on a logarithmic scale. In the box, the curves are amplified in the region between 30 V and 35 V.

Table 1 summarizes the results obtained for the module performance tests at each step, correlating the damage inflicted on the module, the parameters obtained from the I-V curves performed with the solar simulator, and the corresponding value extracted from the dark I-V curves.

Table 1. Parameters obtained from the I-V curves performed with the solar simulator and the corresponding V10 values.

	Step 1	Step 2	Step 3	Step 4	Step 5	Step 6	Step 7
Module Damage	no damage	mallet impact on the frontal face	mallet impact on the frontal face	mallet impact at the corner	mallet impact at the long edge	mallet impact on the back face	walking across the front glass
P_{MAX} (W)	527.5	529.3	527.0	524.8	520.8	515.9	493.1
Vmp (V)	40.88	41.02	40.93	40.90	40.80	40.77	40.76
Imp (A)	12.90	12.90	12.88	12.83	12.77	12.65	12.10
Voc (V)	49.80	49.79	49.81	49.72	49.76	49.67	49.61
Isc (A)	13.62	13.61	13.59	13.58	13.61	13.58	13.52
FF (%)	78	78	78	78	77	76	74
V10	34.56	34.0	34.20	33.59	33.19	32.62	31.84

Figure 10 compares the results obtained in the experiment conducted by Smith and Colvin (2025) with those obtained in the current work. Both results are expressed as relative changes in P_{MAX} versus relative changes in V10. The former was conducted on a PERC full-cell module and the latter on a half-cell module. It can be observed that the relative variation is much more (approximately four times) sensitive for the full-cell module.

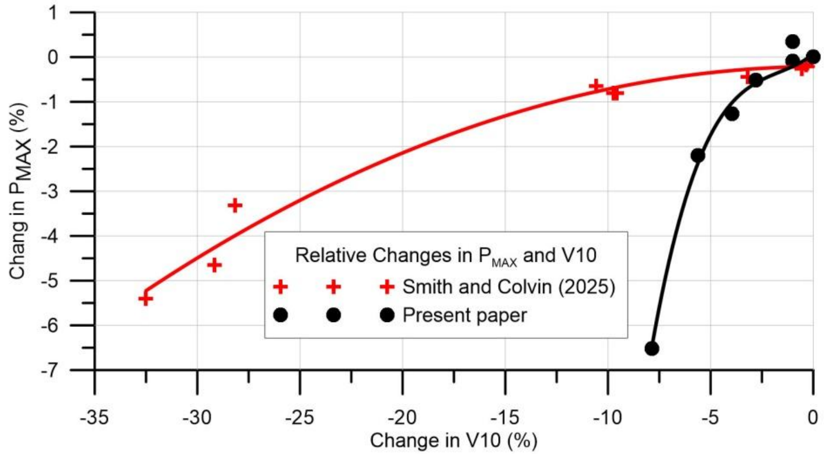

Figure 10. Graph of relative changes comparing the results of Smith and Colvin (2025) and the current work.

6. Conclusions

This work analyzed the variations in experimentally determined characteristic curves, obtained through dark measurements and the flash test, for a half-cell module subjected to mechanical damage of progressive intensities. In conducting this study, the feasibility of utilizing the technique proposed by Smith and Colvin (2025), which they called V10, was also tested. The results demonstrated that the technique can be adopted for half-cell modules, despite showing lower sensitivity regarding the decrease in maximum power. This reduced sensitivity is likely related to the parallel connection of the substrings. Further experiments, utilizing a more representative sample size, are necessary to confirm the repeatability of these results.

7. Acknowledgments

This study was financed in part by the Coordenação de Aperfeiçoamento de Pessoal de Nível Superior - Brasil (CAPES) - Finance Code 001 and National Council for Scientific and Technological Development (CNPq), processo: 306046/2022-9.

8. References

Bosco, N., 2022. Turn Your Half-Cut Cells for a Stronger Module, IEEE Journal of Photovoltaics, Volume 12, DOI: 10.1109/JPHOTOV.2022.3192118.

Bouzidia, K., Chegaara , M.. Aillerieb, M., 2012. Solar cells parameters evaluation from dark I-V characteristics, Energy Procedia 18 , 1601 – 1610, DOI: .1016/j.egypro.2012.06.001.

Fischer, M., Woodhouse, M., Brammer, T. Baliozian, P.,l 2025. International Technology Roadmap for Photovoltaics 16, 2024 Results. VDMA e. V. Photovoltaic Equipment. Frankfurt. Edition May 2025 (itrpv.vdma.org).

Gasparin, F. P., Buhler, A.J.,Rampinelli, G.A. Krenzinger, A., 2016.Statistical analysis of I–V curve parameters from photovoltaic modules. Solar Energy 131 p 30–38.

King, D. L., Hansen, B. R., Kratochvil, J. A., Quintana, M. A., 1997. Dark current-voltage measurements on photovoltaic modules as a diagnostic or manufacturing tool, Conference Record of the Twenty Sixth IEEE Photovoltaic Specialist Conference. DOI: 10.1109/PVSC.1997.654286.

Palmiotti, E. , Springer, M. , Zuboy, M. Silverman, T. , Braid, J. , Jordan, D. , Rabade, S. , Barnes, T., 2025. Growing Panes: Investigating the PV Technology Trends Behind Frequent Early Failures in Modern Glass–Glass Modules. IEEE Journal of Photovoltaics, Vol. 15, DOI: 10.1109/JPHOTOV.2025.3526170.

Smith, Ryan M,. Colvin, Dylan J., 2025. V10: Fixed dark bias current as a photovoltaic module damage assessment matric. Solar Energy, 288, article 113271. DOI: 10.1016/j.solener.2025.113271.

Spataru, Sergiu V., Sera, D., Hacke, P., Kerekes, T., 2015. Fault identification in crystalline silicon PV modules by complementary analysis of the light and dark current-voltage characteristics. Progress in Photovoltaics: Research and Applications. DOI:10.1002/pip.2571.